Electronic Supplementary Information

Hydrolysis of amide bonds in dipeptides and nylon 6 over a ZrO_2 catalyst

Satoshi Tomita,[a] Mizuho Yabushita,[a,*] Yoshinao Nakagawa,[a] Keiichi Tomishige[a,b,*]

[a]*Department of Applied Chemistry, School of Engineering, Tohoku University, 6-6-07 Aoba, Aramaki, Aoba-ku, Sendai, Miyagi 980-8579, Japan*

[b]*Advanced Institute for Materials Research (WPI-AIMR), Tohoku University, 2-1-1 Katahira, Aoba-ku, Sendai, Miyagi 980-8577, Japan*

**Corresponding authors: m.yabushita@tohoku.ac.jp (M.Y.); tomishige@tohoku.ac.jp (K.T.)*

Table S1. Previous reports on catalytic hydrolysis of various peptides.[a]

Entry	Substrate (amount)	Catalyst (amount)	Solvent	Temp. [K]	Time [h]	Conv. [%]	Yield [%]	TOF[b] [h^{-1}]	Ref.
1	Cbz-Gly-Ser-OMe (150 mM)	$Sc(OTf)_3$ (75 mM)	H_2O/EtOH (vol/vol = 1/1)	373	18	n.r.	86[f]	0.096[i]	S1
2	Gly-Gly (2.0 mM)	$K_{15}H[Zr(\alpha_2\text{-}P_2W_{17}O_{61})_2]$ (2 mM)	D_2O (pD = 5.0 by using DCl)	333	900	99	98[g]	0.0050	S2
3	Gly-Phe (10 mM)	$Ce(NH_4)_2(NO_3)_6$ (10 mM)	TRIS buffer (pH 7.0; 0.1 M)	353	24	93	88	0.35 (323 K)	S3
4	Gly-Gly (2 μmol)	MOF-808[c] (2.0 μmol based on Zr_6 cluster)	D_2O (1 mL; pD = 7.4 by using NaOD)	333	4.5	99	99[g]	0.14	S4
5	Hen egg-white lysozyme (0.02 mM)	MOF-808[c] (2.0 μmol based on Zr_6 cluster)	Phosphate buffer (pH 7.4)	333	1–25	n.r.[e]	n.r.[e]	–	S4
6	Gly-Gly (2 μmol)	MIP-201[c] (2.0 μmol based on Zr_6 cluster)	D_2O (1 mL; pD = 7.4 by using NaOD)	333	25	81	80[g]	0.0083	S5
7	Myoglobin (0.02 mM)	MIP-201[c] (2.0 μmol based on Zr_6 cluster)	HEPES buffer (pH 7.4) or H_2O (pH 7.4)	333	1–96	n.r.[e]	n.r.[e]	–	S5
8	Gly-Gly (2 μmol)	NU-1000[c] (2.0 μmol based on Zr_6 cluster)	D_2O (1 mL; pD = 7.4 by using NaOD)	333	220	75	46[g]	0.0017	S6
9	Hen egg-white lysozyme (0.02 mM)	NU-1000[c] (2.0 μmol based on Zr_6 cluster)	H_2O (1 mL)	333	5–72	n.r.[e]	n.r.[e]	–	S6
10	Gly-Gly (2 μmol)	UiO-66[c] (2.0 μmol based on Zr_6 cluster)	D_2O (1 mL; pD = 7.8 by using NaOD)	333	360	66	65[g]	0.0004	S7
11	Hen egg-white lysozyme (0.02 mM)	UiO-66[c] (2.0 μmol based on Zr_6 cluster)	Phosphate buffer (pH 7.4) or H_2O (pH 7.4)	333	0–50	n.r.[e]	n.r.[e]	–	S7
12	Bovine serum albumin (50 pmol)	SP-550C[d] (10 μL of resin slurry)	H_2O (5 μL)	383	20	n.r.[e]	36[h]	–	S8

13	Gly-Gly (2.0 mmol)	m-ZrO_2 (0.10 g (0.81 mmol))	H_2O (5.0 g)	373	24	100	97[g]	1.2	This work
14	Gly-Leu (0.50 mmol)	m-ZrO_2 (0.025 g (0.20 mmol))	H_2O (5.0 g)	373	24	100	95 (Gly) 95 (Leu)	0.59 (Gly) 0.59 (Leu)	This work
15	Gly-Asp (0.50 mmol)	m-ZrO_2 (0.025 g (0.20 mmol))	H_2O (5.0 g)	373	72	100	82 (Gly) 84 (Asp)	0.089 (Gly) 0.079 (Asp)	This work
16	His-Leu (0.50 mmol)	m-ZrO_2 (0.025 g (0.20 mmol))	H_2O (5.0 g)	373	24	100	73 (His) 76 (Leu)	0.44 (His) 0.48 (Leu)	This work

[a]Abbreviations: Cbz = benzyloxycarbonyl; Gly = glycine; Ser = L-serine; OTf = trifluoromethanesulfonate; Phe = L-phenylalanine; Leu = L-leucine; Asp = L-aspartic acid; His = L-histidine; m-ZrO_2 = monoclinic-rich ZrO_2; TRIS = tris(hydroxymethyl)aminomethane hydrochloride; HEPES = 2-[4-(2-hydroxyethyl)-1-piperazinyl]ethanesulfonic acid; n.r. = not reported. [b]Turnover frequency calculated from the initial formation rate of target product (in the case of Gly-Gly, the halved value was used due to the production of two glycine molecules) and mole of metal atoms in each catalyst: TOF [h^{-1}] = (Formation rate of target product [mmol h^{-1}]) / (Mole of metal atoms in each catalyst [mmol]). [c]Metal-organic framework (MOF) consisting of Zr_6 cluster. [d]Cation-exchange resin in H^+-form. [e]Only the data of sodium dodecyl sulfate-polyacrylamide gel electrophoresis (SDS-Page) were reported. [f]Total yield of Cbz-Gly-OH and Cbz-Gly-OEt. [g]Carbon-based yield (unit: %-C). [h]Total yield of amino acids. [i]Calculated from the reaction result shown in this table due to a lack of time course data.

Table S2. Previous reports on catalytic hydrolysis/alcoholysis of aliphatic and aromatic amides.[a]

Entry	Substrate (amount [mmol])	Reaction type	Catalyst (amount)	Solvent[b] (amount)	Additive (amount)	Temp. [K]	Time [h]	Conv. [%]	Yield [%]		TOF[c] [h^{-1}]	Ref.
									Carboxylic acid (or ester)	Amine (or NH_3)		
1	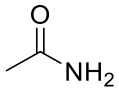 (1)	Hydrolysis	Nb_2O_5 (50 mg (0.19 mmol))	H_2O (5 mmol)	–	Reflux	20	100	97	n.r.	0.21	S9
2	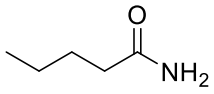 (1)	Alcoholysis	CeO_2 (80 mg (0.46 mmol))	Benzyl alcohol (1 mmol) + mesitylene (1.5 g)	–	438	22	n.r.	95 (ester)	n.r.	7.1	S10
3	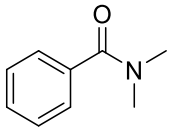 (1)	Alcoholysis	CeO_2 (80 mg (0.46 mmol))	*n*-$C_8H_{17}OH$ (2 mmol)	HY zeolite[e] (0.1 g)	448	36	n.r.	97 (ester)	n.r.	0.20	S11
4	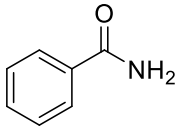 (1)	Alcoholysis	CeO_2 (80 mg (0.46 mmol))	Phenol (1.25 mmol)	–	453	36	100	97 (ester)	n.r.	0.12	S12
5	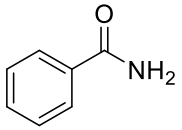 (0.3)	Alcoholysis	MOF-808-P[d] (0.0125 mmol based on Zr_6 cluster)	*n*-C_4H_9OH (0.6 mL)	–	423	24	100	99 (ester)	n.r.	0.50	S13
6	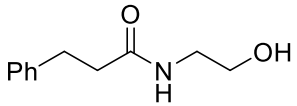 (1)	Alcoholysis	$Zn(OTf)_2$ (0.05 mmol)	*n*-C_4H_9OH (2 mL)	Dimethyl carbonate (2 mmol)	Reflux	45	n.r.	85 (ester)	n.r.	0.38[f]	S14

7	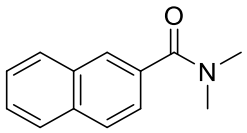 (0.5)	Alcoholysis	$[Mn(acac)(OEt)(EtOH)]_4$ (0.0025 mmol)	*n*-C_4H_9OH (0.25 mL)	Me_2N-phen (0.01 mol)	Reflux	18	n.r.	>99 (ester)	n.r.	2.8[f]	S15
8	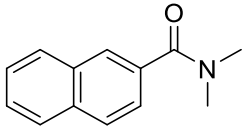 (0.5)	Alcoholysis	$Mn(acac)_2(Me_2$ N-phen) (0.025 mmol)	*n*-C_4H_9OH (0.25 mL)	KOMe (0.025 mmol)	Reflux	12	n.r.	96 (ester)	n.r.	8.6	S16
9	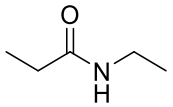 (2.0)	Hydrolysis	m-ZrO_2 (0.10 g (0.81 mmol))	H_2O (10 g)	–	463	120	79	78	76	0.087	This work
10	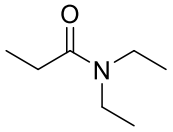 (2.0)	Hydrolysis	m-ZrO_2 (0.10 g (0.81 mmol))	H_2O (10 g)	–	463	168	52	48	50	0.0070	This work

[a]Abbreviations: OTf = trifluoromethanesulfonate; acac = acetylacetonate; OEt = ethoxy; EtOH = ethanol; Me_2N-phen = 4,7-bis(dimethylamino)-1,10-phenanthroline; m-ZrO_2 = monoclinic-rich ZrO_2; OMe = methoxy; n.r. = not reported. [b]In the cases of alcohols and phenol, they behaved as both a reaction solvent and reactant. [c]Turnover frequency calculated from the initial formation rate of carboxylic acid (or ester) and mole of metal atoms in each catalyst: TOF [h^{-1}] = (Formation rate of carboxylic acid (or ester) [mmol h^{-1}]) / (Mole of metal atoms in each catalyst [mmol]). [d]Metal-organic framework (MOF) consisting of Zr_6 cluster. [e]Placed at the upper side of the reaction vessel. [f]Calculated from each reaction result shown in this table due to a lack of time course data.

Table S3. Exemplified previous reports on hydrolysis of nylon 6.[a]

Entry	Substrate (amount [g])	Catalyst (amount [g])	Solvent	Temp. [K]	Time [h]	Conv. [%]	Yield [%]		Ref.
							ε-Caprolactam	ε-Aminocaproic acid	
1	Nylon 6 carpet (180)	–	Steam (1500 kPa, 6 g min^{-1})	613	3	n.r.	90	n.r.	S17
2	Nylon 6 (0.1)	–	H_2O (3.7 mL)	573	1	n.r.	85	3.3	S18
3	MC nylon (1.0)	–	H_2O (30 g)	618	1.3	100	89	0	S19
4	Waste and scrap nylon 6	–	H_2O (nylon 6/H_2O = 1/11 (wt/wt))	573	1	100	92	n.r.	S20
5	Nylon 6	$H_3PW_{12}O_{40}$ (3%)	H_2O (nylon 6/H_2O = 1/15 (wt/wt))	603	1.2	n.r.	78	n.r.	S21
6	Nylon 6 (8.0)	HCl (12 M, 200 mL)	H_2O	382	24	n.r.	n.r.	85[c]	S22
7	MC nylon (1.0)	H-Beta[b] (0.3)	H_2O (39 g)	618	1.2	100	82	n.r.	S23, S24
8	MC nylon (1.0)	Sulfated γ-Al_2O_3-ZrO_2 (0.3)	H_2O (39 g)	618	1.2	n.r.	80	n.r.	S23
9	Nylon 6 (0.23)	m-ZrO_2 (0.10)	H_2O (10 g)	453	16	n.d.	55	33	This work
10	Nylon 6 (0.23)	m-ZrO_2 (0.10)	H_2O (10 g)	503	2	n.d.	81	13	This work
11	Nylon 6 (0.23)	–	H_2O (10 g)	503	2	n.d.	6.5	0.0	This work

[a]Abbreviations: MC = monomer casting; m-ZrO_2 = monoclinic-rich ZrO_2; n.d. = not determined; n.r. = not reported. [b]Si/Al ratio = 12. [c]Isolated yield of ε-aminocaproic acid hydrochloride.

Table S4. List of chemicals used in this study.

Chemical (abbreviation)	Supplier	Purity, concentration, or detailed information
Glycylglycine (Gly-Gly)	Tokyo Chemical Industry	>99.0%
Glycine (Gly)	Tokyo Chemical Industry	>99.0%
Glycine anhydride	Tokyo Chemical Industry	>98.0%
$CaCO_3$	FUJIFILM Wako Pure Chemical	>99.5%
$Zr(OH)_4$	Daiichi Kigenso Kagaku Kogyo	
Glycyl-L-leucine (Gly-Leu)	Peptide Institute	>99.0%
L-Leucine (Leu)	Tokyo Chemical Industry	>99.0%
Glycyl-L-aspartic acid (Gly-Asp)	Sigma-Aldrich	>99.0%
L-Aspartic acid (Asp)	Tokyo Chemical Industry	>99.0%
L-Histidyl-L-leucine (His-Leu)	Peptide Institute	>99.0%
L-Histidine (His)	Tokyo Chemical Industry	>99.0%
N-Ethylpropionamide	Tokyo Chemical Industry	>99.0%
Propionic acid	Tokyo Chemical Industry	>99.0%
Ethylamine	Tokyo Chemical Industry	70 wt%
N,*N*-Diethylpropionamide	Tokyo Chemical Industry	>98.0%
Diethylamine	Tokyo Chemical Industry	>99.0%
Nylon 6	Sigma-Aldrich	Pellets (diameter = 2.2 mm)
ε-Aminocaproic acid	Tokyo Chemical Industry	>98.0%
ε-Caprolactam	Tokyo Chemical Industry	>99.0%
D-Sorbitol	FUJIFILM Wako Pure Chemical	>98.0%
tert-Butyl alcohol	Tokyo Chemical Industry	>99.0%
Glycerol	FUJIFILM Wako Pure Chemical	>99.5%
NaH_2PO_4	FUJIFILM Wako Pure Chemical	>98.0%
Na_2HPO_4	FUJIFILM Wako Pure Chemical	>99.0%
Acetonitrile	Kanto Chemical	>99.9%, HPLC grade

Table S5. List of metal oxides and chemicals tested as catalysts in this study.

Catalyst (abbreviation)	Supplier	Product name or detailed information	Heat-treatment conditions prior to each use		
			Atmosphere	Temp. [K]	Time [h]
Monoclinic-rich ZrO_2 (m-ZrO_2)	Daiichi Kigenso Kagaku Kogyo	RC-100 grade	Air	673–873	3
Tetragonal-rich ZrO_2 (t-ZrO_2)	Prepared by ourselves	Calcination of $Zr(OH)_4$ at 673 K for 3 h in air	–	–	–
CeO_2	Daiichi Kigenso Kagaku Kogyo	HS grade	Air	873	3
MgO	Ube Material Industries	500A	N_2 flow (30 mL min^{-1})	773	3
CaO	Prepared by ourselves	Calcination of $CaCO_3$ at 1173 K for 3 h in air	N_2 flow (30 mL min^{-1})	773	3
Y_2O_3	Kanto Chemical		Air	773	3
La_2O_3	Kanto Chemical		Air	773	3
Pr_6O_{11}	Kanto Chemical		Air	773	3
Sm_2O_3	Kanto Chemical		Air	773	3
Yb_2O_3	Kanto Chemical		Air	773	3
TiO_2	FUJIFILM Wako Pure Chemical	Anatase type	Air	773	3
Nb_2O_5	Catalysis Society of Japan	JRC-NBO-1	Air	773	3
MoO_3	FUJIFILM Wako Pure Chemical		Air	773	3
MnO_2	FUJIFILM Wako Pure Chemical		Air	773	3
Fe_2O_3	FUJIFILM Wako Pure Chemical		Air	773	3
ZnO	Kanto Chemical		Air	773	3
α-Al_2O_3	FUJIFILM Wako Pure Chemical		Air	773	3
SiO_2	Fuji Silysia Chemical	G-6 grade	Air	773	3
SnO_2	Kanto Chemical		Air	773	3

SiO_2-Al_2O_3	Catalysis Society of Japan	JRC-SAH-1, Si/Al = 2	Air	773	3
Beta-type zeolite (Beta)	Tosoh	HSZ-930HOA, Si/Al = 13.5, H-type	Air	773	3
FAU-type zeolite (FAU)	Zeolyst	CBV720, Si/Al = 15, H-type	Air	773	3
Hydrotalcite	FUJIFILM Wako Pure Chemical	$Mg_6Al_2(OH)_{16}CO_3 \cdot 4H_2O$	–	–	–
H_2SO_4	FUJIFILM Wako Pure Chemical	96–98%	–	–	–
NaOH	FUJIFILM Wako Pure Chemical	>97%	–	–	–

Table S6. Detailed data of Fig. S2 (hydrolysis of Gly-Gly in the presence of different amount of CaO).[a]

Entry	Time	Amount of CaO		Conv.	Yield [%-C]		Bal.[c]
	[h]	[g]	[mmol]	[%]	Glycine	Glycine anhydride	[%]
1[b]	4	0	0	0	0	0	101
2		0.025	0.45	1.0	0.6	1.0	101
3		0.050	0.89	3.8	0.8	1.3	98
4		0.075	1.3	23	24	0	102
5		0.10	1.8	38	38	0	100
6		0.13	2.2	39	40	0	101
7[b]	8	0	0	0	0	0	100
8		0.025	0.45	4.4	0.3	2.1	98
9		0.050	0.89	4.8	1.5	2.4	99
10		0.075	1.3	31	30	0	100
11		0.10	1.8	63	63	0	100
12		0.13	2.2	65	67	0	102

[a]Reaction conditions: Gly-Gly 2.0 mmol; CaO 0–0.13 g; H_2O 5.0 g; 353 K; 4 or 8 h; Ar. [b]Operated without catalyst in air. [c]Balance.

The hydrolysis of Gly-Gly was operated in the presence of different amount of CaO for 4 h or 8 h (Table S6). Neither 0.025 g nor 0.050 g of CaO was not effective for the hydrolysis of Gly-Gly regardless of the reaction times (entries 2, 3, 8, and 9). These results could result from the neutralization of strongly basic Ca species by acidic functional group (*i.e.*, carboxyl group) of Gly-Gly. The larger amount of CaO (≥0.075 g) proceeded with the hydrolysis of Gly-Gly (entries 4–6 and 10–12), yet 0.10 g and 0.13 g of CaO offered almost the same reaction results (entry 5 *vs.* entry 6 and entry 11 *vs.* entry 12). This unprecedented trend upon the amount of CaO might be again connected to the neutralization of strongly basic species by carboxylic acids involved in both unreacted Gly-Gly and produced glycine (the progress of Gly-Gly hydrolysis increases the number of carboxyl group in a reaction mixture since two glycine molecules are generated from one Gly-Gly molecule). Altogether, CaO was not as an effective catalyst as m-ZrO_2 in the hydrolysis of Gly-Gly.

Table S7. Detailed data of Fig. 2 (time courses of Gly-Gly hydrolysis over m-ZrO_2 catalyst at different temperatures).[a]

Enrty	Temp. [K]	Time [h]	Conv. [%]	Yield [%-C]		Bal.[b] [%]
				Glycine	Glycine anhydride	
1	333	8	15	13	1.6	100
2		24	37	31	2.1	97
3		48	57	52	3.5	99
4		72	69	64	4.2	99
5		96	78	72	4.8	99
6		120	85	78	4.3	97
7	353	2	20	21	1.9	103
8		4	43	40	2.8	101
9		8	65	57	4.9	98
10		24	91	83	5.7	99
11		48	98	91	4.4	98
12		72	100	95	3.2	98
13		96	100	96	2.4	99
14		120	100	95	1.9	97
15	373	0.5	26	25	2.3	102
16		1	53	47	4.9	99
17		1.5	68	59	6.0	97
18		2	82	74	6.9	98
19		4	98	89	6.6	98
20		8	99	94	4.8	100
21		24	100	97	1.6	99

[a]Reaction conditions: Gly-Gly 2.0 mmol; m-ZrO_2 (calcined at 673 K) 0.10 g; H_2O 5.0 g; 333–373 K; 0.5–120 h. [b]Balance.

Table S8. Surface acidity and basicity of fresh and spent m-ZrO_2 catalysts.

Entry	m-ZrO_2	S_{BET}[a] [m^2 g^{-1}]	Desorbed amount of NH_3[b] [μmol g^{-1}]			Desorbed amount of CO_2[b] [μmol g^{-1}]			Conv.[c] [%]	Yield[c] [%-C]		Bal.[c,d] [%]
			383–773 K	773–1173 K	Total	383–773 K	773–1173 K	Total		Glycine	Glycine anhydride	
1	Fresh (1st run)	85	275	34	309	190	14	204	43	40	2.8	101
2	After 2nd run	84	n.d.	n.d.	n.d.	n.d.	n.d.	n.d.	39	35	3.5	99
3	After 3rd run	82	n.d.	n.d.	n.d.	n.d.	n.d.	n.d.	33	26	3.7	97
4	After 3rd run + calcination[e]	84	276	46	322	145	46	191	26	23	3.3	101

[a]BET specific surface area. [b]Total desorbed amount of each probe molecule in each TPD profile (Fig. S8). [c]Results of Gly-Gly hydrolysis (the data for entry 1 are the same as those of m-ZrO_2 in Tables 1 and 2). Reaction conditions: Gly-Gly 2.0 mmol; m-ZrO_2 (calcined at 673 K) 0.10 g; H_2O 5.0 g; 353 K; 4 h. [d]Balance. [e]Calcination conditions: air; 673 K; 3 h.

Table S9. Detailed data of Fig. S9A (time course for the hydrolysis of glycyl-L-leucine (Gly-Leu) over m-ZrO_2 catalyst).[a]

Entry	Time [h]	Conv. [%]	Yield [%]	
			Glycine	L-Leucine
1	0.25	4	3.5	3.9
2	0.5	9	11	11
3	1	25	24	26
4	2	61	58	57
5	4	75	75	77
6	8	96	88	91
7	24	100	95	95

[a]Reaction conditions: glycyl-L-leucine 0.50 mmol; m-ZrO_2 (calcined at 673 K) 0.025 g; H_2O 5.0 g; 373 K; 0.25–24 h.

Table S10. Detailed data of Fig. S9B (time course for the hydrolysis of glycyl-L-aspartic acid (Gly-Asp) over m-ZrO_2 catalyst).[a]

Entry	Time [h]	Conv. [%]	Yield [%]	
			Glycine	L-Aspartic acid
1	1	11	2.9	3.0
2	2	24	6.9	7.3
3	4	38	15	13
4	8	74	31	31
5	24	100	53	53
6	48	100	75	73
7	72	100	82	84

[a]Reaction conditions: glycyl-L-aspartic acid 0.50 mmol; m-ZrO_2 (calcined at 673 K) 0.025 g; H_2O 5.0 g; 373 K; 1–72 h.

Table S11. Detailed data of Fig. S9C (time course for the hydrolysis of L-histidyl-L-leucine (His-Leu) over m-ZrO_2 catalyst).[a]

Entry	Time [h]	Conv. [%]	Yield [%]	
			L-Histidine	L-Leucine
1	0.25	15	4.9	5.3
2	0.5	25	8.3	8.5
3	1	39	18	20
4	4	80	53	58
5	8	94	65	69
6	24	100	73	76
7	48	100	70	73

[a]Reaction conditions: L-histidyl-L-leucine 0.50 mmol; m-ZrO_2 (calcined at 673 K) 0.025 g; H_2O 5.0 g; 373 K; 0.25–48 h.

Table S12. The data of Gly-Gly hydrolysis over m-ZrO_2 catalyst under the same conditions as substrate scope of dipeptides.[a]

Entry	Time [h]	Conv. [%]	Yield [%-C]		Bal.[b] [%]
			Glycine	Glycine anhydride	
1	0.25	15	16	2.2	103
2	0.33	30	28	3.3	102
3	0.5	39	38	4.2	103

[a]Reaction conditions: Gly-Gly 0.50 mmol; m-ZrO_2 (calcined at 673 K) 0.025 g; H_2O 5.0 g; 373 K; 0.25–0.5 h. [b]Balance.

Table S13. Detailed data of Fig. S10 (time course of *N*-ethylpropionamide hydrolysis over m-ZrO_2 catalyst).[a]

Entry	Time [h]	Conv. [%]	Yield [%]		Balance of each moiety [%]	
			Propionic acid	Ethylamine	Carboxylic acid	Amine
1	0	6	2.6	2.6	97	97
2	8	35	31	32	96	97
3	24	54	49	49	94	94
4	48	67	65	65	98	97
5	72	76	74	75	98	99
6	96	74	71	71	96	96
7	120	79	78	76	99	97

[a]Reaction conditions: *N*-ethylpropionamide 2.0 mmol; m-ZrO_2 (calcined at 673 K) 0.10 g; H_2O 10 g; 463 K; 0–120 h.

Table S14. Detailed data of Fig. S11 (time course of *N*,*N*-diethylpropionamide hydrolysis over m-ZrO_2 catalyst).[a]

Entry	Time [h]	Conv. [%]	Yield [%]		Balance of each moiety [%]	
			Propionic acid	Diethylamine	Carboxylic acid	Amine
1	24	11	8.0	8.6	97	97
2	48	20	15	17	95	97
3	120	41	35	37	94	96
4	144	47	41	43	94	96
5	168	52	48	50	96	98

[a]Reaction conditions: *N*,*N*-diethylpropionamide 2.0 mmol; m-ZrO_2 (calcined at 673 K) 0.10 g; H_2O 10 g; 463 K; 0–168 h.

Table S15. Comparison of catalytic activity between m-ZrO_2 and Nb_2O_5 in the hydrolysis of *N*-ethylpropionamide.[a]

Entry	Catalyst	Conv. [%]	Yield [%]		Balance of each moiety [%]	
			Propionic acid	Ethylamine	Carboxylic acid	Amine
1	None	6.3	3.4	3.5	97	97
2	m-ZrO_2	35	31	32	96	97
3	Nb_2O_5	9.2	6.2	5.7	97	96

[a]Reaction conditions: *N*-ethylpropionamide 2.0 mmol; m-ZrO_2 (calcined at 673 K) or Nb_2O_5 0.10 g; H_2O 10 g; 463 K; 8 h.

Table S16. Detailed data of Fig. S12 (time courses of nylon 6 hydrolysis over m-ZrO_2 catalyst at different reaction temperatures).[a]

Entry	Temp. [K]	Time [h]	Yield [%]			Bal.[b] [%]
			ε-Caprolactam	ε-Aminocaproic acid	Oligomers	
1	453	0	3.2	1.8	2.9	7.8
2		4	26	22	32	80
3		8	43	31	20	95
4		12	49	32	14	95
5		16	55	33	8.9	97
6	503	0	23	6.8	13	43
7		0.5	63	13	15	91
8		1	69	14	8.6	92
9		2	81	13	2.2	96
10[c]	503	2	6.5	0.0	4.6	11

[a]Reaction conditions: nylon 6, 0.23 g (corresponding to 2.0 mmol of monomeric unit); m-ZrO_2 (calcined at 673 K) 0.10 g; H_2O 10 g; 453 or 503 K; 0–16 h. [b]Balance. [c]No catalyst.

Table S17. Conversion of ε-caprolactam in the presence of m-ZrO_2 catalyst at different temperatures.[a]

Entry	Temp. [K]	Amount of m-ZrO_2 [g]	Time [h]	Yield [%]			Bal.[b] [%]
				ε-Caprolactam (unreacted substrate)	ε-Aminocaproic acid	Oligomers	
1	453	0.10	16	53	36	7.8	97
2		0.10	32	52	37	8.6	97
3		0.30	16	53	37	9.0	100
4	503	0.10	2	80	15	4.2	100
5		0.10	4	76	21	2.5	99
6		0.30	2	80	16	2.3	98

[a]Reaction conditions: ε-caprolactam 2.0 mmol; m-ZrO_2 (calcined at 673 K) 0.10 or 0.30 g; H_2O 10 g; 453 or 503 K; 2–32 h. [b]Balance.

The reaction data for the conversion of ε-caprolactam in the presence of m-ZrO_2 catalyst (Table S17) allowed to estimate the equilibrium yields of ε-caprolactam and ε-aminocaproic acid at 453 K and 503 K. Due to the consistency among entries 1–3 as well as entries 4–6, the molar ratios of ε-caprolactam to ε-aminocaproic acid, ~1.5 and ~5.3, are the equilibrium compositions at 453 K and 503 K. In other words, the amount of ε-caprolactam becomes higher at the higher reaction temperature of 503 K, which supports the reaction data summarized in Tables 4 and S16 and Fig. S12.

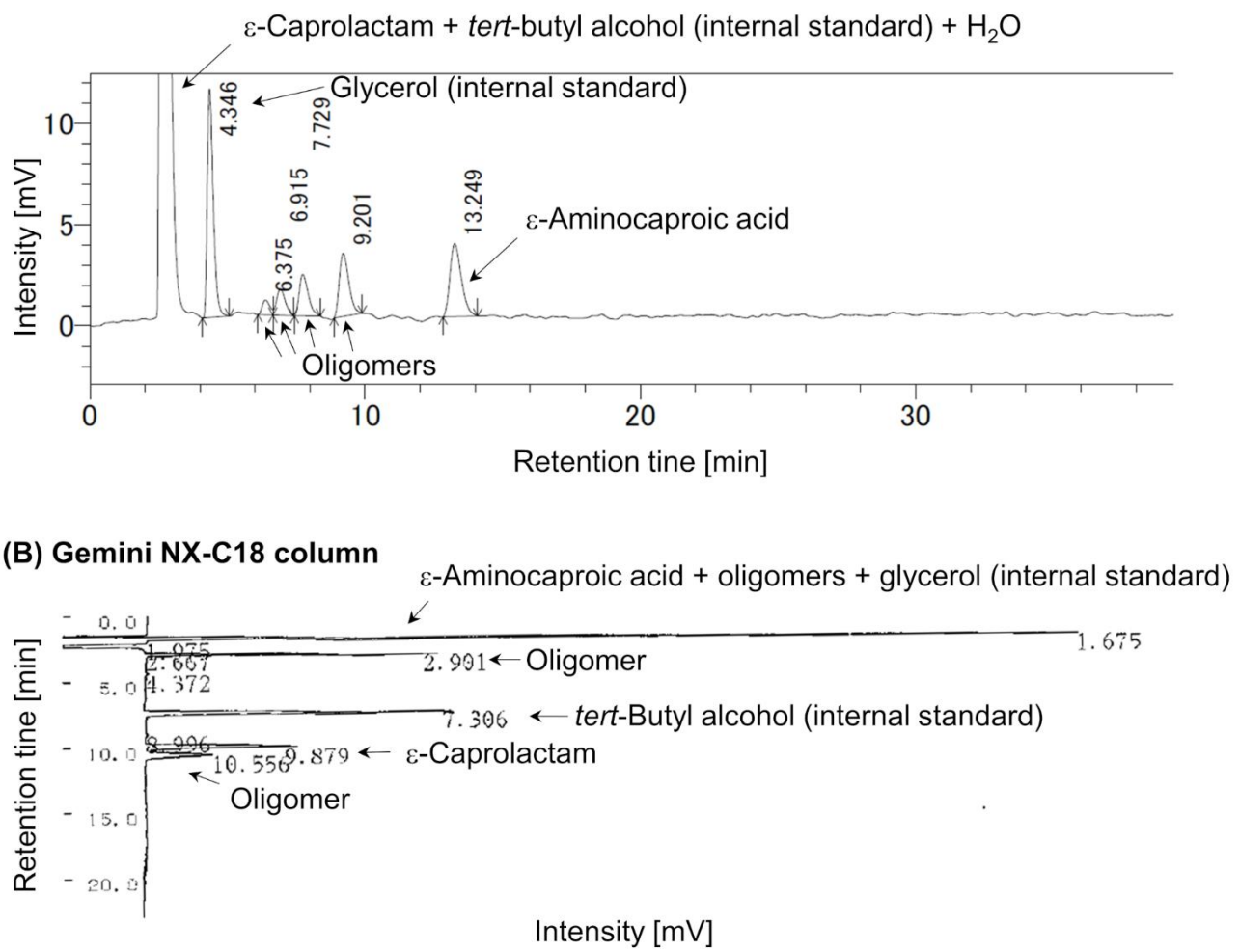

Fig. S1. Typical HPLC charts of the reaction mixture after the hydrolysis of nylon 6 over m-ZrO_2 catalyst operated at 453 K for 4 h (Table S16, entry 2): (A) NH2P-50 4E column; (B) Gemini NX-C18 column. Reaction conditions: nylon 6, 0.23 g (corresponding to 2.0 mmol of monomeric unit); m-ZrO_2 (calcined at 673 K) 0.10 g; H_2O 10 g; 453 K; 4 h.

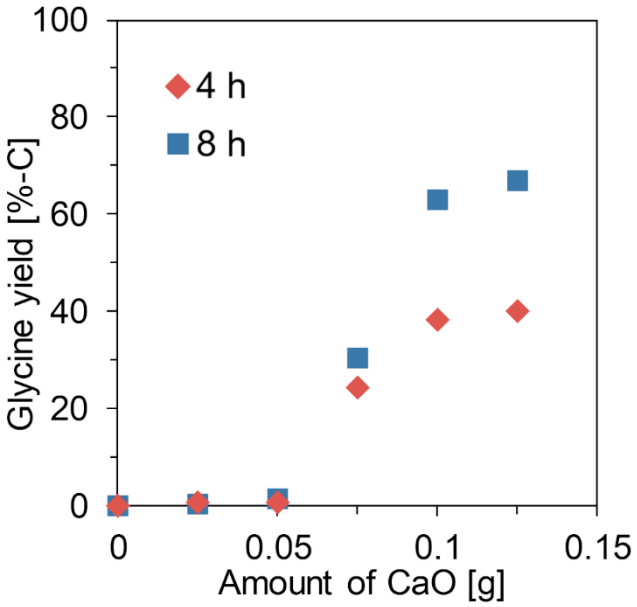

Fig. S2. Hydrolysis of Gly-Gly in the presence of different amount of CaO.
Reaction conditions: Gly-Gly 2.0 mmol; CaO 0–0.125 g; H_2O 5.0 g; 353 K; 4 or 8 h; Ar (in the absence of catalyst, the reactions were operated in air).
The detailed data are shown in Table S6.

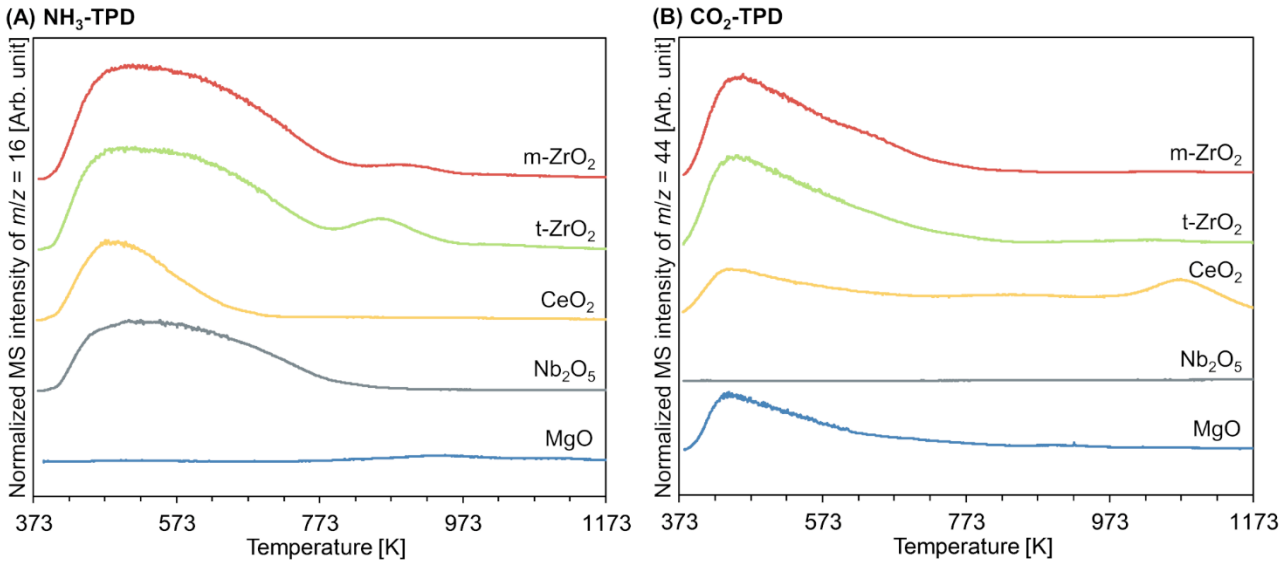

Fig. S3. (A) NH_3-TPD and (B) CO_2-TPD profiles for various metal oxides. The intensity was normalized by the sample amount and calibration factor. The quantification data are summarized in Table 2.
Pretreatment conditions: metal oxide 0.30 g; Ar 50 mL min^{-1}; 673 K, 1 h. For MgO, prior to this standard pretreatment, the sample was heat-treated in an Ar flow (30 mL min^{-1}) at 773 K for 3 h.
Adsorption conditions: (step 1) NH_3/Ar (5.0 vol%) or CO_2/Ar (10 vol%) 50 mL min^{-1}, 373 K, 30 min; (step 2) Ar 50 mL min^{-1}, 373 K, 30 min.
Desorption conditions: Ar 30 mL min^{-1}; 10 K min^{-1}; 373–1173 K.

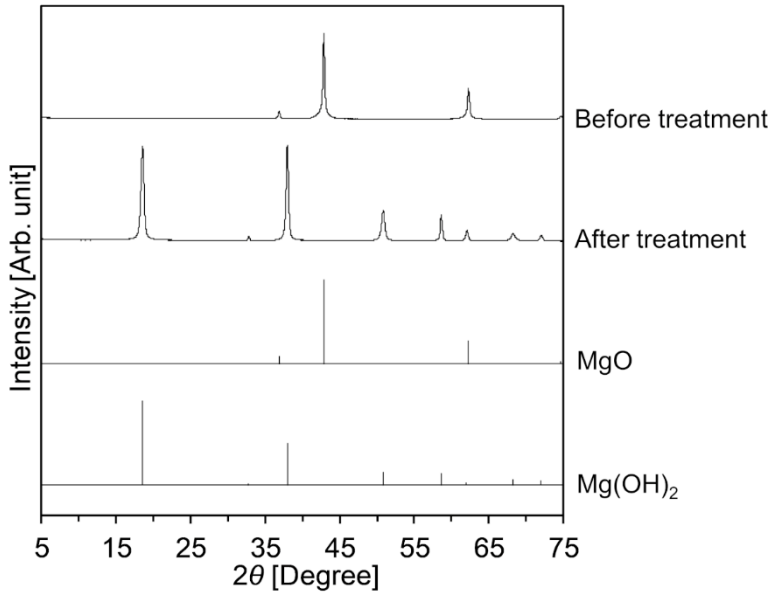

Fig. S4. XRD patterns of MgO before/after the hydrothermal treatment at 353 K.
Treatment conditions: MgO 0.10 g; H_2O 5.0 g; 353 K; 4 h; operated in Ar.
References: cubic MgO = ICSD card #9863; trigonal $Mg(OH)_2$ = ICSD card #79031.

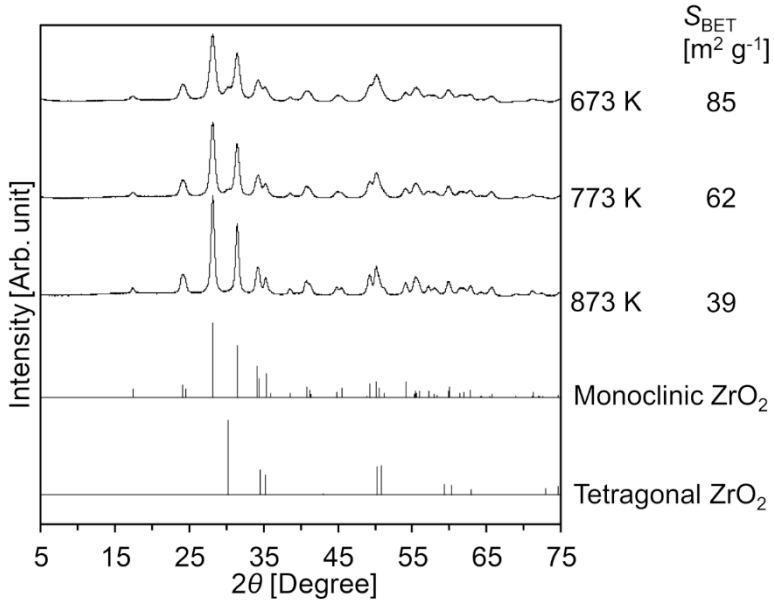

Fig. S5. XRD patterns of m-ZrO_2 samples calcined at different temperatures (673, 773, and 873 K).
References: monoclinic ZrO_2 = ICSD card #18190; tetragonal ZrO_2 = ICSD card #68781.

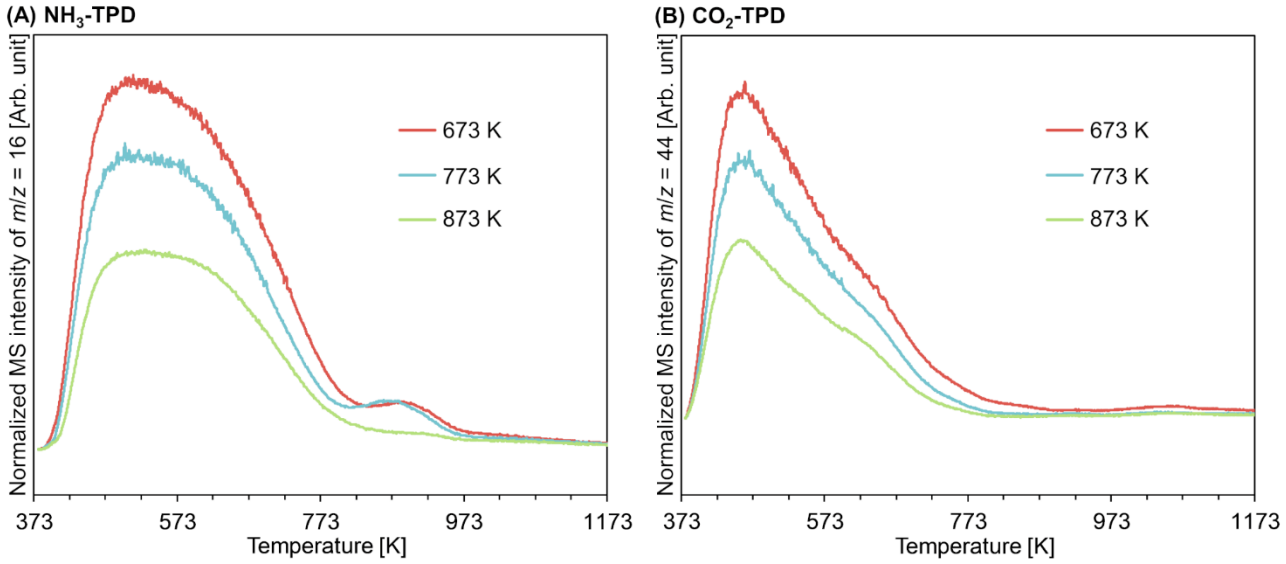

Fig. S6. (A) NH_3-TPD and (B) CO_2-TPD profiles for m-ZrO_2 samples calcined at different temperatures (673, 773, and 873 K). The intensity was normalized by the sample amount and calibration factor. The quantification data are summarized in Table 3.

Pretreatment conditions: m-ZrO_2 0.30 g; Ar 50 mL min^{-1}; 673 K, 1 h.

Adsorption conditions: (step 1) NH_3/Ar (5.0 vol%) or CO_2/Ar (10 vol%) 50 mL min^{-1}, 373 K, 30 min; (step 2) Ar 50 mL min^{-1}, 373 K, 30 min.

Desorption conditions: Ar 30 mL min^{-1}; 10 K min^{-1}; 373–1173 K.

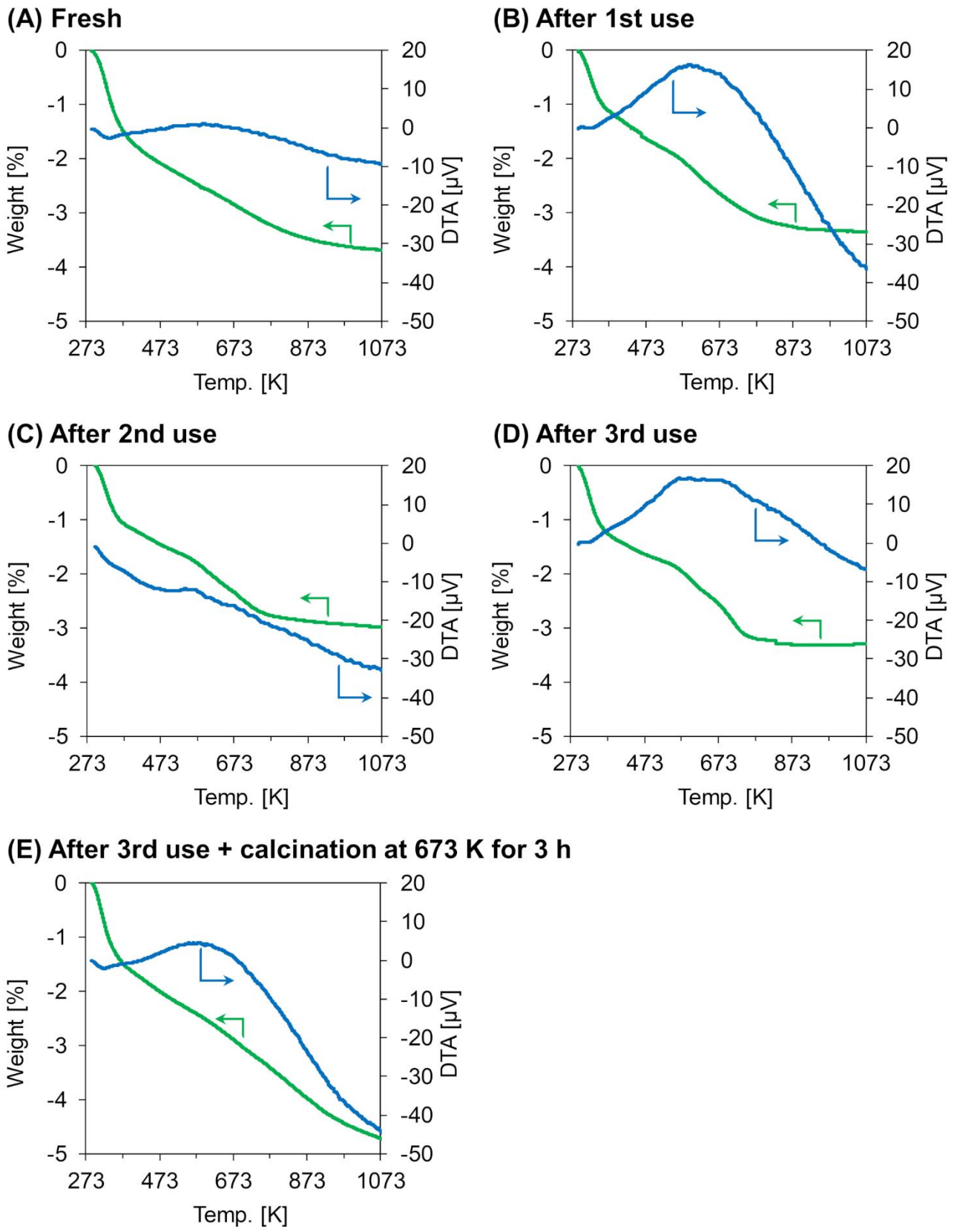

Fig. S7. TG-DTA profiles for fresh and spent m-ZrO_2 catalysts. (A) Fresh, (B) After 1st use, (C) After 2nd use, (D) After 3rd use, and (E) After 3rd use + calcination at 673 K for 3 h.

Reaction conditions: Gly-Gly 2.0 mmol; m-ZrO_2 (calcined at 673 K) 0.10 g; H_2O 5.0 g; 353 K; 4 h.

The reaction data are shown in Fig. 3 and Table S8.

Analytical conditions: sample *ca.* 10 mg; air flow 30 mL min^{-1}; ramp rate 10 K min^{-1}.

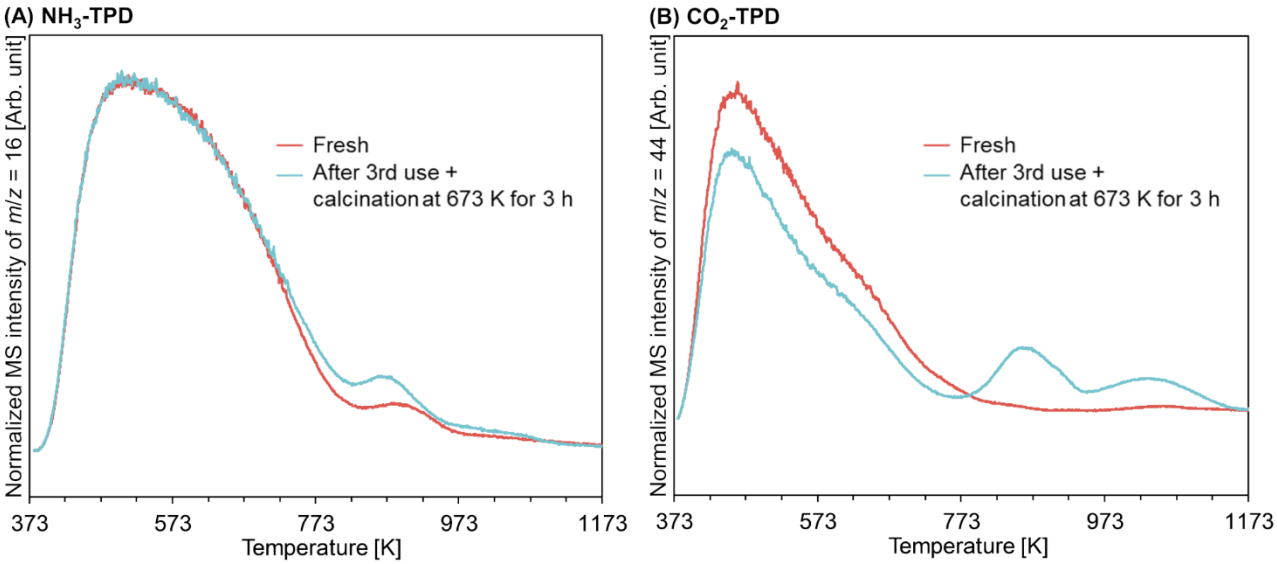

Fig. S8. (A) NH_3-TPD and (B) CO_2-TPD profiles for fresh and spent m-ZrO_2 catalysts. The intensity was normalized by the sample amount and calibration factor. The quantification data are summarized in Table S8. The fresh catalyst was prepared via the calcination at 673 K.

Pretreatment conditions: m-ZrO_2 0.30 g; Ar 50 mL min^{-1}; 673 K, 1 h.

Adsorption conditions: (step 1) NH_3/Ar (5.0 vol%) or CO_2/Ar (10 vol%) 50 mL min^{-1}, 373 K, 30 min; (step 2) Ar 50 mL min^{-1}, 373 K, 30 min.

Desorption conditions: Ar 30 mL min^{-1}; 10 K min^{-1}; 373–1173 K.

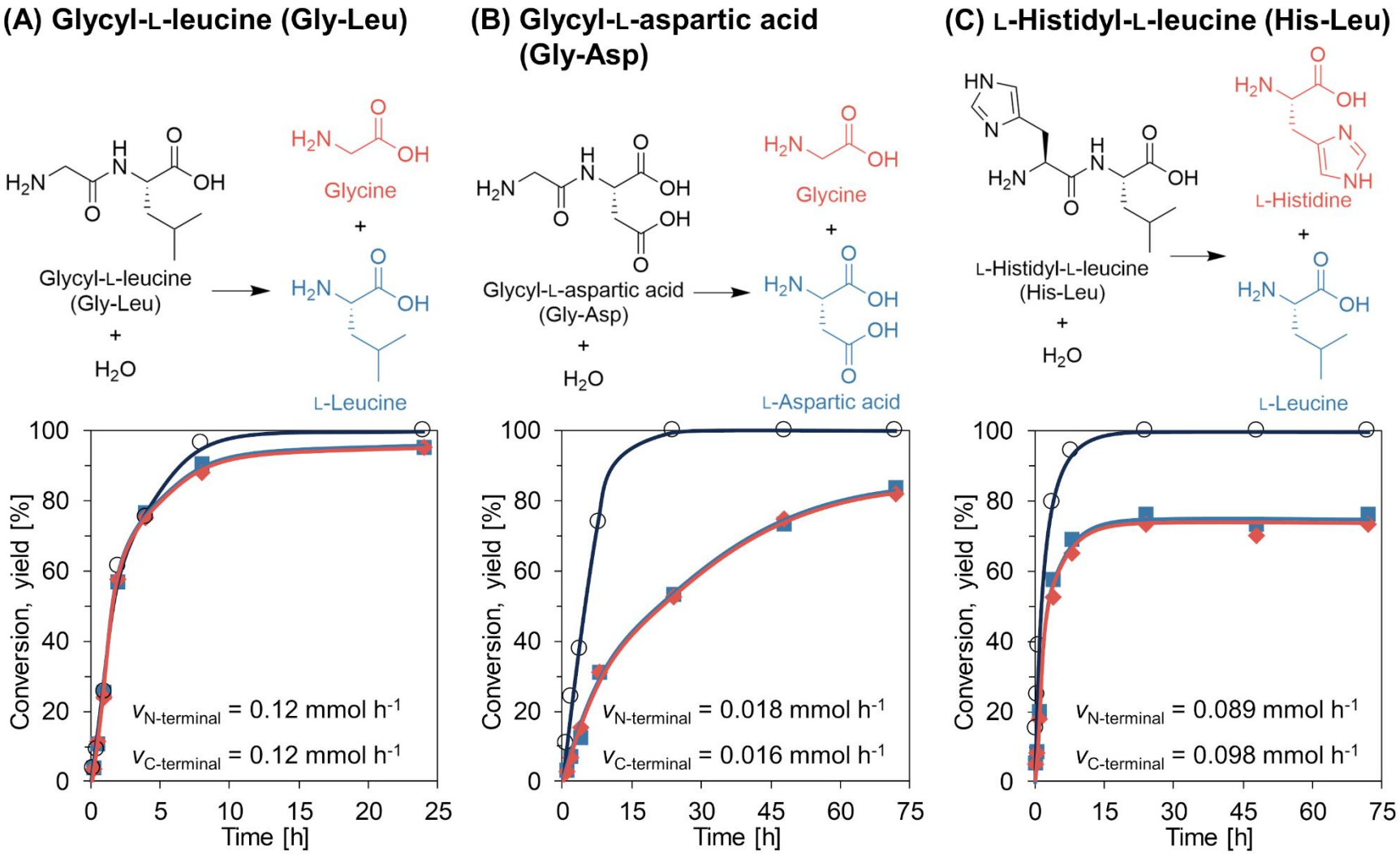

Fig. S9. Time courses for the hydrolysis of various dipeptides over m-ZrO_2 catalyst. Each formation rate of N-terminal/C-terminal amino acid (v [mmol h^{-1}]) was calculated from the initial slope within the conversion range below 40%.

Legends: white circles = conversion of dipeptide; red diamonds = yield of N-terminal amino acid; blue squares = yield of C-terminal amino acid.

Reaction conditions: dipeptide 0.50 mmol; m-ZrO_2 (calcined at 673 K) 0.025 g; H_2O 5.0 g; 373 K; 0.25–72 h.

The detailed data are shown in Tables S9–S11.

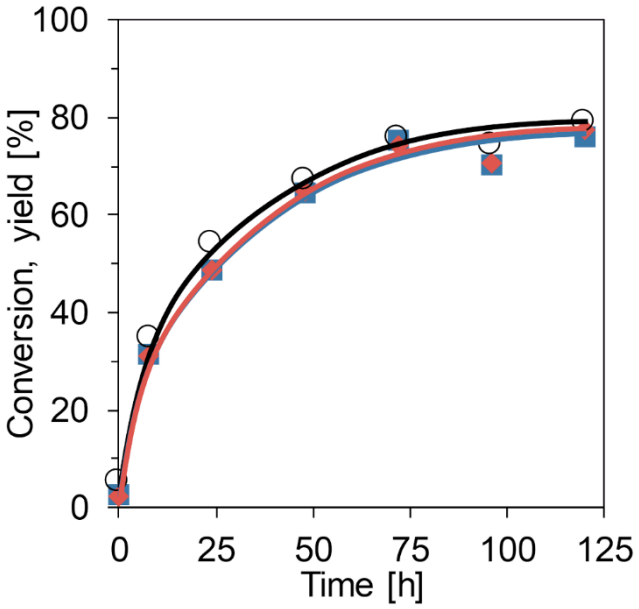

Fig. S10. Time course of *N*-ethylpropionamide hydrolysis over m-ZrO_2 catalyst.
Legends: white circles = conversion; red diamonds = yield of propionic acid; blue squares = yield of ethylamine.
Reaction conditions: *N*-ethylpropionamide 2.0 mmol; m-ZrO_2 (calcined at 673 K) 0.10 g; H_2O 10 g; 463 K; 0–120 h.
The detailed data are shown in Table S13.

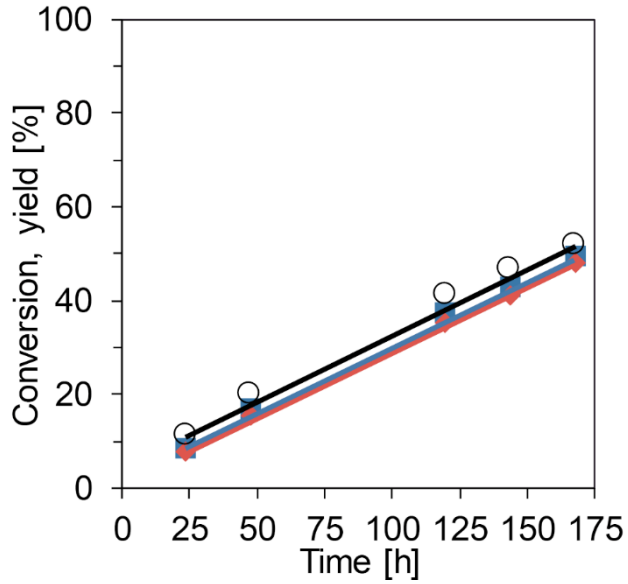

Fig. S11. Time course of *N*,*N*-diethylpropionamide hydrolysis over m-ZrO_2 catalyst.
Legends: white circles = conversion; red diamonds = yield of propionic acid; blue squares = yield of diethylamine.
Reaction conditions: *N*,*N*-diethylpropionamide 2.0 mmol; m-ZrO_2 (calcined at 673 K) 0.10 g; H_2O 10 g; 463 K; 0–168 h.
The detailed data are shown in Table S14.

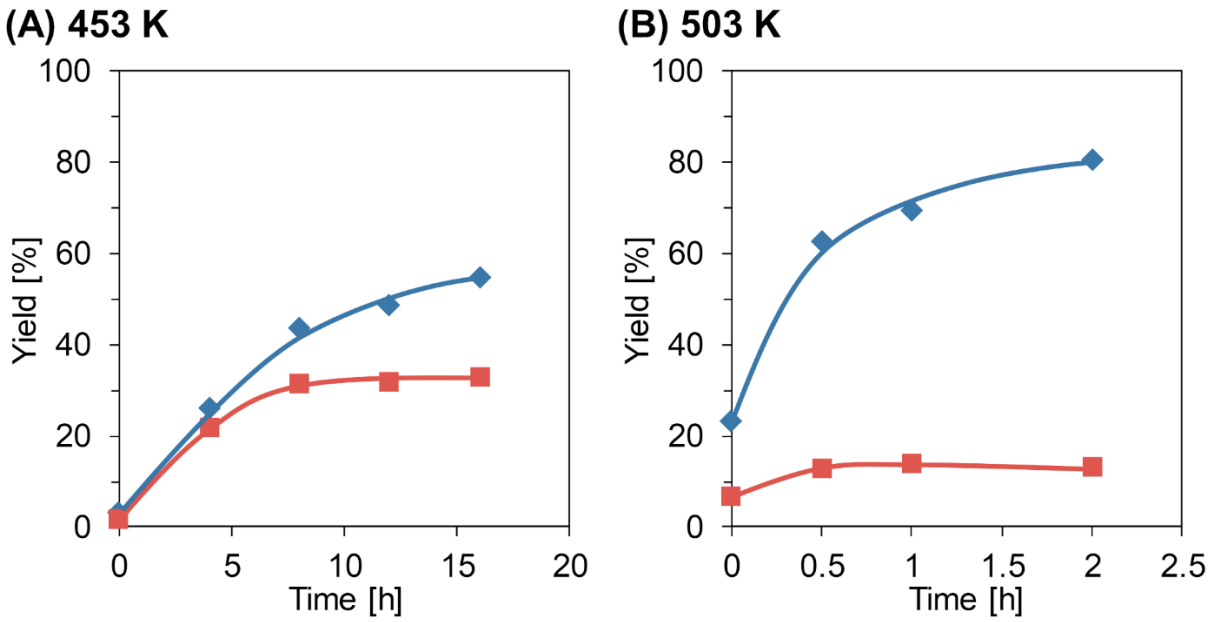

Fig. S12. Time courses of nylon 6 hydrolysis over m-ZrO_2 catalyst at different reaction temperatures: (A) 453 K; (B) 503 K.

Legends: blue diamonds = yield of ε-caprolactam; red squares = yield of ε-aminocaproic acid.

Reaction conditions: nylon 6, 0.23 g (corresponding to 2.0 mmol of monomeric unit); m-ZrO_2 (calcined at 673 K) 0.10 g; H_2O 10 g; 453 or 503 K; 0–16 h.

The detailed data are shown in Table S16.

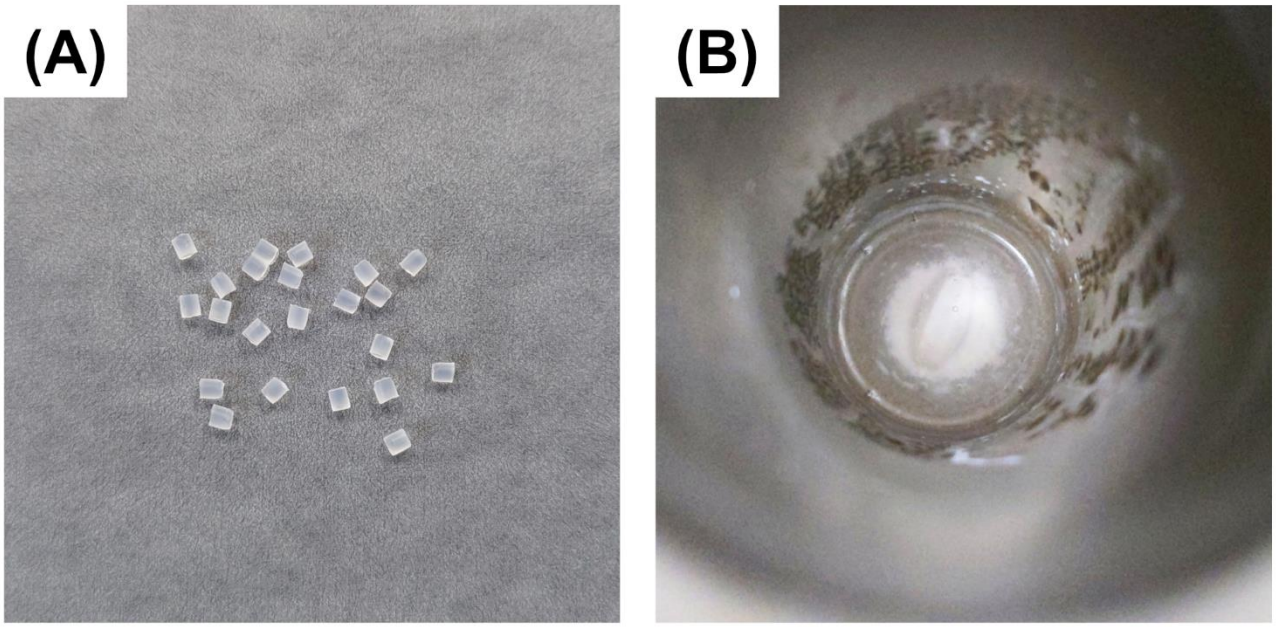

Fig. S13. Photos of (A) nylon 6 (as-received from the supplier) and (B) inside of the autoclave just after the reaction at 453 K for 0 h (*i.e.*, the reactor was cooled down soon after its inner temperature reached 453 K).

Reaction conditions for figure B: nylon 6, 0.23 g (corresponding to 2.0 mmol of monomeric unit); m-ZrO_2 (calcined at 673 K) 0.10 g; H_2O 10 g; 453 K; 0 h.

Supplementary references

S1. J. Ni, Y. Sohma and M. Kanai, *Chem. Commun.*, 2017, **53**, 3311–3314.

S2. G. Absillis and T. N. Parac-Vogt, *Inorg. Chem.*, 2012, **51**, 9902–9910.

S3. T. Takarada, M. Yashiro and M. Komiyama, *Chem. Eur. J.*, 2000, **6**, 3906–3913.

S4. H. G. T. Ly, G. Fu, A. Kondinski, B. Bueken, D. De Vos and T. N. Parac-Vogt, *J. Am. Chem. Soc.*, 2018, **140**, 6325–6335.

S5. S. Wang, H. G. T. Ly, M. Wahiduzzaman, C. Simms, I. Dovgaliuk, A. Tissot, G. Maurin, T. N. Parac-Vogt and C. Serre, *Nat. Commun.*, 2022, **13**, 1284.

S6. A. Loosen, F. de Azambuja, S. Smolders, J. Moons, C. Simms, D. De Vos and T. N. Parac-Vogt, *Chem. Sci.*, 2020, **11**, 6662–6669.

S7. H. G. T. Ly, G. Fu, F. de Azambuja, D. De Vos and T. N. Parac-Vogt, *ACS Appl. Nano Mater.*, 2020, **3**, 8931–8938.

S8. A. Masuda and N. Dohmae, *Anal. Chem.*, 2010, **82**, 8939–8945.

S9. S. M. A. H. Siddiki, M. N. Rashed, A. S. Touchy, M. A. R. Jamil, Y. Jing, T. Toyao, Z. Maeno and K. Shimizu, *Catal. Sci. Technol.*, 2021, **11**, 1949–1960.

S10. S. M. A. H. Siddiki, A. S. Touchy, M. Tamura and K. Shimizu, *RSC Adv.*, 2014, **4**, 35803–35807.

S11. T. Toyao, M. N. Rashed, Y. Morita, T. Kamachi, S. M. A. H. Siddiki, M. A. Ali, A. S. Touchy, K. Kon, Z. Maeno, K. Yoshizawa and K. Shimizu, *ChemCatChem*, 2019, **11**, 449–456.

S12. M. N. Rashed, S. M. A. H. Siddiki, A. S. Touchy, M. A. R. Jamil, S. S. Poly, T. Toyao, Z. Maeno and K. Shimizu, *Chem. Eur. J.*, 2019, **25**, 10594–10605.

S13. B. Villoria-del-Álamo, S. Rojas-Buzo, P. García-García and A. Corma, *Chem. Eur. J.*, 2021, **27**, 4588–4598.

S14. Y. Kita, Y. Nishii, T. Higuchi and K. Mashima, *Angew. Chem. Int. Ed.*, 2012, **51**, 5723–5726.

S15. H. Nagae, T. Hirai, D. Kato, S. Soma, S. Akebi and K. Mashima, *Chem. Sci.*, 2019, **10**, 2860–2868.

S16. T. Hirai, D. Kato, B. K. Mai, S. Katayama, S. Akiyama, H. Nagae, F. Himo and K. Mashima, *Chem. Eur. J.*, 2020, **26**, 10735–10742.

S17. M. Braun, A. B. Levy and S. Sifniades, *Polym.-Plast. Technol. Eng.*, 1999, **38**, 471–484.

S18. T. Iwaya, M. Sasaki and M. Goto, *Polym. Degrad. Stab.*, 2006, **91**, 1989–1995.

S19. W. Wang, L. Meng and Y. Huang, *Polym. Degrad. Stab.*, 2014, **110**, 312–317.

S20. H. Hu, Q. Xu, L. Sun, R. Zhu, T. Gao, Y. He, B. Ma, J. Yu and X. Wang, *ACS Appl. Polym. Mater.*, 2023, 5, 751–763.

S21. J. Chen, Z. Li, L. Jin, P. Ni, G. Liu, H. He, J. Zhang, J. Dong and R. Ruan, *J. Mater. Cycles Waste Manag.*, 2010, **12**, 321–325.

S22. X.-X. Yuan, Q. Zhou, X.-Y. Li, P. Yang, K.-K. Yang and Y.-Z. Wang, *Polym. Degrad. Stab.*, 2014, **109**, 171–174.

S23. W. Wang, L. Meng, K. Leng and Y. Huang, *Polym. Degrad. Stab.*, 2017, **136**, 112–120.

S24. W. Wang, L. Meng, J. Yu, F. Xie and Y. Huang, *J. Anal. Appl. Pyrolysis*, 2017, **125**, 218–226.